A DNA-based molecular motor that can navigate a network of tracks.

Shelley F. J. Wickham[1], Jonathan Bath[1], Yousuke Katsuda[2], Masayuki Endo[3,4], Kumi Hidaka[2] , Hiroshi Sugiyama,[2,3,4*] and Andrew J. Turberfield[1*]

[1]University of Oxford, Department of Physics, Clarendon Laboratory, Parks Road, Oxford OX1 3PU, UK. [2]Department of Chemistry, Graduate School of Science, Kyoto University, Kitashirakawa-oiwakecho, Sakyo-ku, Kyoto 606-8502, Japan. [3]Institute for Integrated Cell-Material Sciences (iCeMS), Kyoto University, Yoshida-ushinomiyacho, Sakyo-ku, Kyoto 606-8501, Japan. [4]CREST, Japan Science and Technology Corporation (JST), Sanbancho, Chiyoda-ku, Tokyo 102-0075, Japan.

Synthetic molecular motors can be fuelled by the hydrolysis[1-4] or hybridization[5-11] of DNA. Such motors can move autonomously[1-4,7-11] and programmably[12], and long-range transport has been observed on linear tracks[13,14]. It has also been shown that DNA systems can compute[8,15-18]. Here we report a synthetic DNA-based system that integrates long-range transport and information processing. We show that the path of a motor through a network of tracks containing four possible routes can be programmed using instructions that are added externally or carried by the motor itself. When external control is used we find that 87% of the motors follow the correct path; 71% of the motors follow the correct path when internal control is used. Programmable motion will allow the development of computing networks, molecular systems that can sort and process cargos according to instructions that they carry, and assembly lines[19,20] that can be reconfigured dynamically in response to changing demands.

A network of branching tracks was constructed on a rectangular DNA origami tile[21]. Each tile, 100 nm × 70 nm, is assembled from a single-stranded circular template that is hybridized to and cross-linked by 216 short staple strands to form a raft of 24 parallel DNA double helices. The ends of the staples lie on an approximately hexagonal grid, with 6 nm spacing, on one face of the tile. The tracks consist of single-stranded DNA anchorages ('stators') extending from the 5' ends of selected staples[14]. The track architecture is shown in Figure 1a and Supplementary Figures 1 and 2. The first section of the track is perpendicular to the origami helices; it then splits into two branches, both at ~60° to the initial direction (the first layer of control comprising a single node). Two special control stators are positioned directly downstream from the node. Unique address and toehold[22] sequences allow these control stators to be selectively blocked and unblocked to direct a motor down a particular path (Figure 1c). The branching motif is repeated (the second layer of control comprising two nodes) to give four possible routes through the network (Figure 1a). Motors must take 7 steps to traverse a one-layer track and 12 to traverse a two-layer track.

We use a shorthand (*x,y*) for a program of motion that involves taking direction *x* at the first node and *y* at the second, where *x* = {L,R} instructs the motor to turn {left, right} at the first node. Stators are labeled according to their position in the programmed sequence of motion: for example, S_{11}(R,L) is the 11th stator along the path that turns right at the first node and left at the second. Addition of instruction strand i(L,-) unblocks control stator S_5(L) at the first junction and directs the motor down the left-hand path. Similarly, strand i(R,-) unblocks S_5(R) and directs the motor to the right. In two-layer tracks, the junction sequences at the second nodes are repeated: control stators S_{11}(L,L) and S_{11}(R,L) are both unblocked by control strand i(-,L), and S_{11}(L,R) and S_{11}(R,R) are unblocked by i(-,R). The four final stators are reached by unique paths through the network prescribed by the four possible combinations of instruction strands: [i(L,-)+i(-,L)] leads to destination S_{13}(L,L); [i(L,-)+i(-,R)] leads to S_{13}(L,R); etc.

The motor[3] consists of a single strand of DNA that is complementary to a domain common to each stator. The motor-stator duplex contains the recognition site of a nicking restriction enzyme that catalyses hydrolysis of the stator, leading to the dissociation of the cut fragment and exposure of a 6-nucleotide (nt) toehold[22] that initiates migration of the motor onto an adjacent intact stator[5] (Figure 1c). The motor is initially hybridized to the first stator (S_1), which is incorporated in the tile in a final

assembly step[14]. To assist the loading process, stator S_1 is designed to hybridize to an additional 2 nt of the motor. All other stators (not just the control stators) are initially occupied by 'block' strands. Block strands prevent binding of the motor to a stator: they hybridize to an identifying address domain at the top of the stator and a short section of the motor-binding domain (10 nt for control stators and 6 nt for all other stators). They also incorporate a single-stranded toehold[22] that facilitates their removal by addition of a complementary 'unblock' strand with a matching address domain (Figure 1c). All generic stators, but only selected control stators, are unblocked before the motor is activated by addition of enzyme. The blocking strand binding domain does not extend far enough into the enzyme recognition site to allow blocked stators to be cut. Stators at track ends contain a single-base mismatch in the enzyme recognition site that prevents cleavage and thus captures the motor when it reaches the end of the track.

Ensemble fluorescence measurements were used to observe transport of a fluoresence-quenching cargo molecule, attached to the motor, past fluorophores positioned along the track. One-layer tracks were labeled at S_1, S_8(L) and S_8(R) with fluorophores F_1, F_8(L) and F_8(R), respectively. Partial tracks containing only one branch were used to confirm that the motor behaves on tracks with 60° bends as on straight tracks of the same length (Supplementary Figure 3). Figure 2 shows time-dependent fluorescence signals from branched tracks. In all cases, F_1 intensity increases immediately on addition of enzyme, indicating motion away from S_1. Quenching of fluorophores F_8 indicates accumulation of the motor at the track ends. When instruction i(x) is added before transport is initiated, fluorescence from the intended destination $F_8(x)$ is quenched strongly, while fluorescence from the other track-end label is largely unchanged (65% of motors have reached the end of the track within 200 minutes, of which 76% reach the correct destination–see Supplementary Information Tables 2 and 3). When both instruction strands are added, F_8(L) and F_8(R) are quenched equally (28% of motors reach the left end, 28% the right). These results do not depend on the choice of fluorophores at the track ends (Supplementary Figure 4). This demonstrates that the dominant path taken by the motor is determined by the instructions added, and that when both paths at the junction are open there is no bias between them. Leakage of motor into the 'wrong' path is observed: this is significantly reduced when the control stator for each track branch is repeated at position S_6 (of the 56% of motors that reach the end of the track within 200 minutes, 87% reach the correct destination, Figure 2). Motors can cross a 12 nm gap in the track at a much slower rate[14], and may leak past the block by stepping directly onto the next available downstream stator. Twin-block tracks increase the required step-size to 18 nm, reducing the leakage rate further[14]. If both downstream paths are blocked, the motor is not trapped indefinitely (Supplementary Figure 5): it either leaks forward through the blocked stators or diffuses back over the cut stators towards S_1. Diffusion is slow compared to enzyme-driven stepping[14], and can be neglected if at least one downstream path is unblocked.

Fluoresence measurements were used to observe motor movement along a two-layer track with twin blocking stators at each node. (The additional control sequence was tested in separate experiments: Supplementary Figure 6). Tiles labeled with F_7(R) at intermediate stator S_7(R) on the first right branch, and with F_{13}(R,L) and F_{13} (R,R) at two of the four track ends, were tested with all four instruction sets. The experiment was then repeated with tiles labeled at F_7(R), F_{13}(L,L) and F_{13}(L,R). The combined

results are shown in Figure 3. A dip in F_7(R) fluorescence, indicating passage of the motor along the right branch at the first node, is observed if and only if the instruction for the first node is i(R,-). The results for the four F_{13} fluorophores confirm that, in each case, the dominant destination of the motor corresponds to the instructions given (67% of motors that reach the end of the track within 200 minutes have reached the correct destination). The second instruction strand operates on both nodes in the second layer, and directs the motor even if it takes the incorrect path at the first node. For example, addition of program (R,L), results in strong quenching of F_{13}(R,L) as expected (65% of motors reaching the end within 200 minutes are at S_{13}(R,L)), but of those motors that take the wrong path at the first node, 69% are directed correctly to S_{13}(L,L).

The conclusion that the path chosen by the motor is determined by the control strands is supported by atomic force microscopy (AFM) imaging. Motor strands modified with biotin were labeled with streptavidin after execution of the program, then imaged by AFM to determine the motor location. Representative images are shown in Figure 3 iii. Histograms of final motor positions are consistent with the programs loaded (Figure 3 iv).

In the experiments described above, broadcast instructions are supplied to an ensemble of motors in solution by diffusion. A potentially richer set of behaviors is possible if instructions are carried by the motors themselves. Such a system is outlined in Figure 4a. The block strand was designed with looped secondary structure in order to impede hybridization with the complementary unblock strand: this was found to reduce the uncatalysed reaction rate less significantly than was expected[23] so a short splice strand was added to the unblock strand to form a two-strand loop complex that further impedes the reaction (Figure 4a, Supplementary Figure 7). The motor incorporates an additional single-stranded DNA domain that is designed to catalyse hybridization between a specific pair of block and unblock strands, opening only one branch of the track. Unblock strands for all control stators are added before motion is initiated but the unblocking reaction is only catalysed when the motor reaches the selected junction (Supplementary Figure 9). Fluorescence measurements show operation of the motor-catalysed system on a single-layer track (Figure 4 and Supplementary Figure 8). A significant bias is observed towards the branch encoded by the catalytic sequence carried by the motor (59% for the instruction (R), 70% for the instruction (L)). A motor can catalyse more than one unblocking reaction: for instruction (R), a twin block causes a small decrease in the fraction of motor reaching the end of the track (from 37% for a single block to 33% for a twin block), and a more significant increase in the bias towards the correct destination (from 59% to 70%) for motors that do reach the end of the track. For instruction (L), the twin block results in a decrease in the fraction of the motor that reaches the end of the track (from 52% to 39%) but little or no change in the bias towards the correct destination (70%). The trade off between increasing the fidelity with which instructions are interpreted and decreasing the fraction of motors that traverse the track within a given time must be considered when optimizing this system.

These results demonstrate that a DNA motor can be routed through a spatial network of bifurcating tracks. The path taken at a junction can be externally controlled or programmed by information carried by the motor itself (with 87% and 71% of the cargo routed correctly for external and internal control respectively). Track elements

can be repeated in series to improve efficiency and re-used at different branch points. More complex track networks could be produced by concatenating origami tiles to form larger structures[24-27]. This work represents a significant advance in the creation of programmable and adaptable molecular systems. The capacity to control routing decisions locally, by means of signals carried by the motors that they control, is a particularly significant step: molecular transporters can already operate without the need for external control[1-4,7-14]; they can now process information autonomously, Individual molecular robotic systems that to respond to local stimuli and pass control signals to each other could lead, for example, to the development of responsive systems for distributed drug manufacture and release. These characteristics provide the elements of control required to implement Petri-Net-style computation[28]; they also permit complex collective behaviours such as those that underlie 'social' robotics[29].

1. Yin, P., Yan, H., Daniell, X. G., Turberfield, A. J. & Reif, J. H. A unidirectional DNA walker that moves autonomously along a DNA track. *Angew. Chem. Int. Edn* **43,** 4906-4911 (2004).

2. Tian, Y., He, Y., Peng, Y. & Mao, C. A DNA enzyme that walks processively and autonomously along a one-dimensional track. *Angew. Chem. Int. Edn* **44,** 4355-4358 (2005).

3. Bath, J., Green, S. J. & Turberfield, A. J. A free-running DNA motor powered by a nicking enzyme. *Angew. Chem. Int. Edn* **44,** 4358-4361 (2005).

4. Pei, R. et al., Behaviour of polycatalytic assemblies in a substrate-displaying matrix. *J. Am. Chem. Soc.* **128,** 12693-12699 (2006).

5. Shin, J. -S. & Pierce, N. A. A synthetic DNA walker for molecular transport. *J. Am. Chem. Soc.* **126,** 10834-10835 (2004).

6. Sherman, W. B. & Seeman, N. C. A precisely controlled DNA biped walking device. *Nano Lett.* **4,** 1203-1207 (2004).

7. S. Venkataraman, S., Dirks, R. M., Rothemund, P. W. K., Winfree, E. & Pierce, N. A. An autonomous polymerization motor powered by DNA hybridization. *Naure Nanotech.* **2,** 490-494 (2007).

8. Yin, P., Choi, H. M., Calvert, C. R. & Pierce, N. A. Programming biomolecular self-assembly pathways. *Nature* **451,** 318-322 (2008).

9. Green, S. J., Bath, J. & Turberfield, A. J. Coordinated chemomechanical cycles: a mechanism for autonomous molecular motion. *Phys. Rev. Lett.* **101,** 238101 (2008).

10. Bath, J. Green, S. J., Allen, K. E. & Turberfield, A. J. Mechanism for a directional, processive and reversible DNA motor. *Small* **5,** 1513-1516 (2009).

11. Omabegho, T., Sha, R. & Seeman, N. C. A bipedal Brownian motor with coordinated legs. *Science* **324,** 67-71 (2009).

12. Muscat, R. A., Bath, J. & Turberfield, A. J. A Programmable Molecular Robot. *Nano Lett.* **11**, 982–987 (2011).

13. Lund, K. *et al.*, Molecular robots guided by prescriptive landscapes. *Nature* **465**, 206-210 (2010).

14. Wickham, S. F. J., Endo, M., Katsuda, Y., Hidaka, K., Bath, J., Sugiyama, H. & Turberfield, A. J. Direct observation of stepwise movement of a synthetic molecular transporter. *Nature Nanotech.* **6**, 166-169 (2011).

15. Stojanovic, M. N., Mitchell, T. E. and Stefanovic, D. Deoxyribozyme-based logic gates. *J. Am. Chem. Soc.* **124**, 3555–3561 (2002).

16. Zhang, D. Y., Turberfield, A. J., Yurke, B. & Winfree, E. Engineering entropy-driven reactions and networks catalyzed by DNA. *Science* **318**, 1121-1125 (2007).

17. Benenson, Y., Gil, B., Adar, U. B.-D. R. and Shapiro, E. An autonomous molecular computer for logical control of gene expression. *Nature* **429**, 423– 429 (2004).

18. Qian, L. & Winfree, E. Scaling Up Digital Circuit Computation with DNA Strand Displacement Cascades. *Science* **332**, 1196-1201 (2011).

19. He, Y. and Liu, D. R. Autonomous multistep organic synthesis in a single isothermal solution mediated by a DNA walker. *Nature Nanotech.* **5**, 778–782 (2010).

20. Gu, H., Chao, J., Xiao, S. J. & Seeman, N. C. A proximity-based programmable DNA nanoscale assembly line. *Nature* **465**, 202-205 (2010).

21. Rothemund, P. W. K. Folding DNA to create nanoscale shapes and patterns. *Nature* **440,** 297-302 (2006).

22. Yurke, B. & Mills Jr, A. P. Using DNA to power nanostructures. *Genetic Programming and Evolvable Machines* **4,** 111-122 (2003).

23. Turberfield, A. J. et al. DNA fuel for free-running nanomachines. *Phys. Rev. Lett.* **90,** 118102 (2003).

24. Douglas, S. M. et al., Self-assembly of DNA into nanoscale three-dimensional shapes. *Nature* **459,** 414-418 (2009).

25. Endo, M., Sugita, T., Katsuda, Y., Hidaka, K. & Sugiyama, H. Programmed-Assembly System Using DNA Jigsaw Pieces**.** *Chem. Eur. J.* **16,** 5362-5368 (2010).

26. Rajendran, A., Endo, M., Katsuda, Y., Hidaka, K. & Sugiyama H. Programmed Two-Dimensional Self-Assembly of Multiple DNA Origami Jigsaw Pieces. *ACS Nano* **5**, 665–671 (2011).

27. Liu, W., Zhong, H., Wang, R. & Seeman, N. C. Crystalline Two-Dimensional DNA-Origami Arrays. *Angew. Chem. Int. Edn* **50**, 264-267 (2011).

28. Petri, C. A. Kommunikation mit Automaten. Bonn: Institut fur Instrumentelle Mathematik, Schriften des IIM Nr. 3 (1962).

29. Krieger, M. J. B., Billeter, J. B. & Keller, L. Ant-like task allocation and recruitment in cooperative robots. *Nature* **406**, 992-995 (2000).

Acknowledgements. This work was supported by the Engineering and Physical Sciences Research Council (EP/G037930/1), the Clarendon Fund, the Oxford–Australia Scholarship Fund, the CREST of JST and a Grant-in-Aid for Science Research from the Ministry of Education, Culture, Sports, Science and Technology, Japan.

Author contributions. Experiments were designed by S.W. with input from J.B. and A.J.T. Ensemble fluorescence experiments were carried out by S.W. in the laboratory of A.J.T.. AFM experiments were done by M.E., Y.K. and K.H in the laboratory of H.S. The manuscript was written by S.W., J.B., H.S. and A.J.T.

Additional information. The authors declare no competing financial interests. Supplementary information accompanies this paper at www.nature.com/naturenanotechnology. Reprints and permission information is available online at http://npg.nature.com/reprintsandpermissions/. Correspondence and requests for materials should be addressed to H.S. and A.J.T.

Figure 1. Programmed route on branching tracks. a The DNA track network is assembled on a rectangular DNA origami substrate. Selective displacement of blocking strands from junction stators (coloured crosses) opens just one path. The motor (black circle) travels down the open path, destroying the track behind it. **b** Tracks decorated with excess motor visualized by AFM (scale bars 50 nm). A reference marker (black square) is used to confirm the orientation of the track **c** 'Block' strands with unique address domains (magenta/green) prevent the motor (black) from stepping when it reaches a junction. The selected path is unblocked by an instruction strand which hybridizes to the toehold on the selected block strand (green) to initiate a strand displacement reaction that removes it from the stator. The motor can then step to the unblocked stator. The resulting duplex contains a new recognition site for the nicking enzyme: enzyme cleavage of the stator, and subsequent dissociation of the cut stator fragment, generates a 6-nt toehold that initiates migration of the motor onto the next intact stator. Repetition of this cycle of step and cut drives the motor along the programmed path.

Figure 2: Externally controlled DNA motor on a single-layer track. The motor transports a fluorescence quencher past fluorophores F_1, F_8(R) and F_8(L), labeling stators at the beginning and ends of the track. **a** Addition of instruction i(R), unblocking the control stator on the right-hand branch, directs the motor to S_8(R) and results in strong quenching of F_8(R). **b** i(L) directs the motor to S_8(L), where it quenches F_8(L). **c** If both paths are open the motor quenches F_8(R) and F_8(L) equally. Leakage into the wrong branch is decreased for 'twin-block' tracks, where each control stator is repeated at successive positions downstream from the node.

Figure 3. Controlled motion on a two-layer track. Four instruction strands are used to control the path taken by the motor, which transports a fluorescence quencher past fluorophores positioned along the track. **a** Time-dependent fluoresence intensities (**i**) and diagram showing programmed route (**ii**) on addition of instruction set (R,R). The right hand path at both junctions is opened, and the motor is directed to stator S_{13}(R,R) where it quenches fluorophore F_{13}(R,R). **iii** AFM image of a streptavidin-labeled motor (M) showing its final location at the programmed track end, □ indicates a reference marker. A height profile of this image is shown in Supplementary Figure 10. **iv** Histogram showing proportions of motors detected by AFM at each track end (number of tiles counted, N = 21). Similar results indicate correctly programmed motion for the other instruction sets: **b** (R,L), N=22; **c** (L,R), N=21 and **d** (L,L), N=25. A transient dip in F_7(R) is seen only if the instruction set contains (R,-). (Scale bars 20 nm.)

Figure 4. Internally programmed motion on a single-layer track. a The motor carries a catalytic domain that can only unblock a path with complementary address domains (magenta). A 6 nt toehold carried by the motor (M) initiates a strand exchange reaction that partially displaces the blocking strand (B) from the adjacent stator revealing a domain that was previously sequestered in a loop. The open loop interacts with the unblock•splice (U•S) complex to nucleate a four-arm Holliday junction. Resolution of the junction removes the unblocking strand from the stator leaving the shorter splice domain in its place. Note that the nicking enzyme places some restriction on the design of the blocking and splice strands: the block•stator duplex must not contain a recognition sequence and the splice•stator duplex must reveal a toehold to allow the motor to step. Transfer of the motor to the unblocked stator proceeds as described in Fig. 1 except that 2 nt of the 6 nt toehold remain obscured by the splice domain. **c** Motor(R) carries the instruction to open the right-hand path, and is directed to S_8(R), quenching F_8(R). **d** Motor(L) quenches F_8(L). **e** A motor carrying no catalytic instruction domain is split between the two paths. Leakage into the wrong state is decreased for twin-block tracks, which have two independently blocked stators on each path downstream from the node.

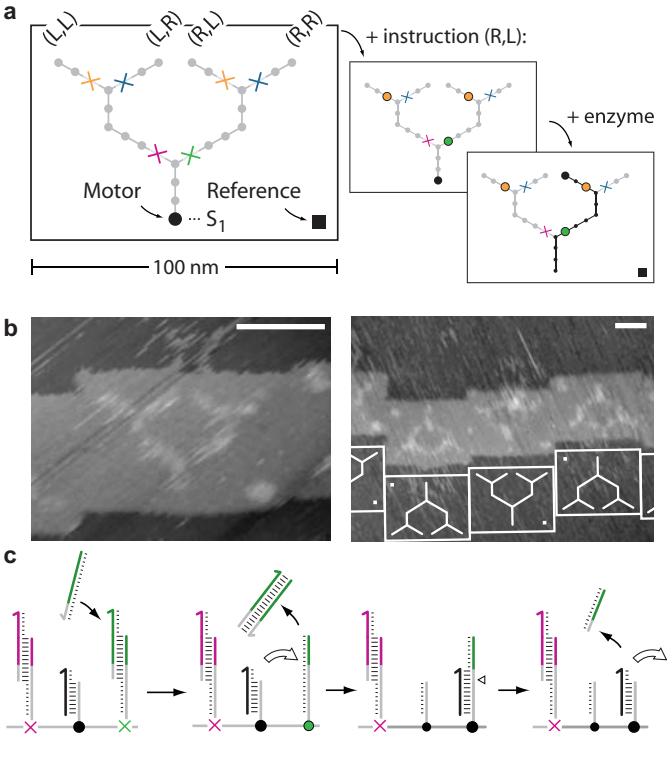
a
(L,L)
(L,R)
(R,L)
(R,R)
+ instruction (R,L):
+ enzyme
Motor
Reference
S1
100 nm
b
c

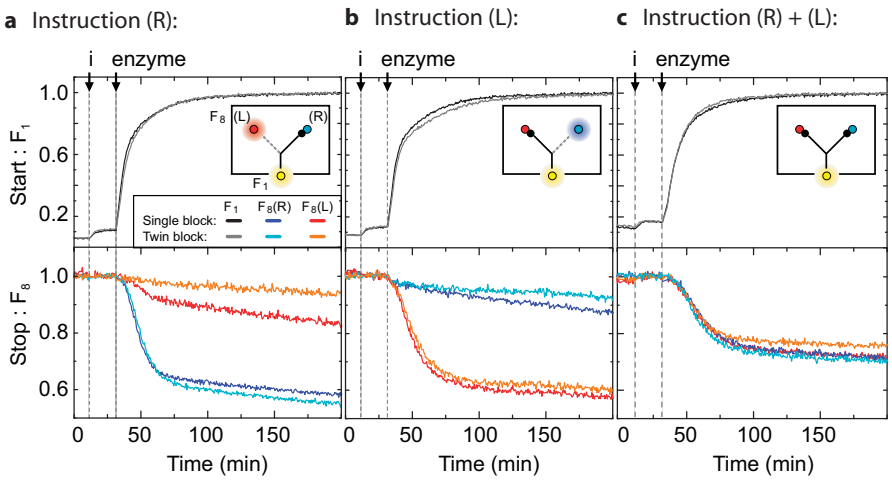
a Instruction (R):
b Instruction (L):
c Instruction (R) + (L):
i
enzyme
Start : F1
Stop : F8
1.0
0.6
0.2
0.8
F8
(L)
(R)
F1
Single block:
Twin block:
F1
F8(R)
F8(L)
0
50
100
150
Time (min)

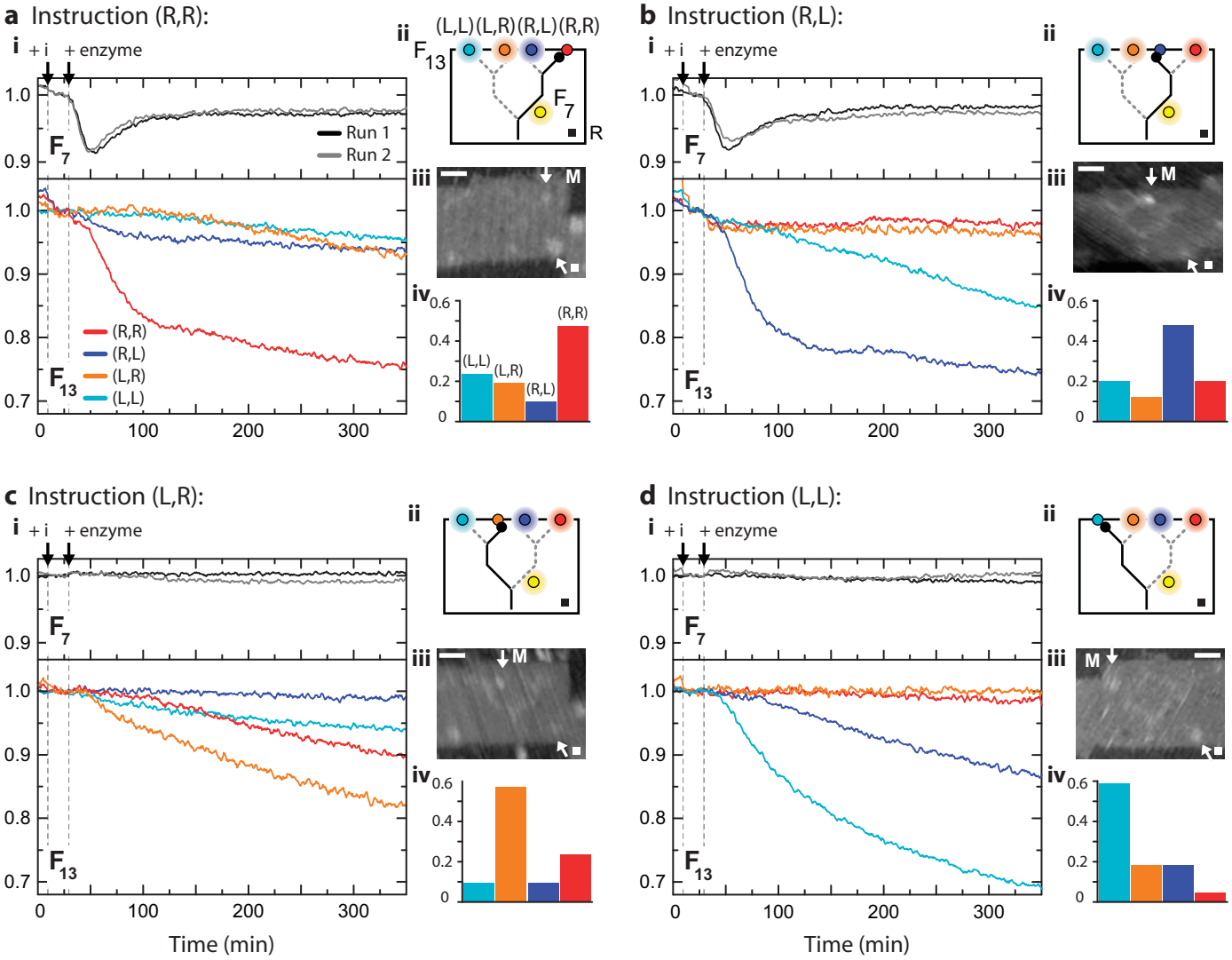
a Instruction (R,R):
b Instruction (R,L):
c Instruction (L,R):
d Instruction (L,L):
i
+ i
+ enzyme
ii
iii
iv
(L,L)(L,R)(R,L)(R,R)
F13
F7
R
M
Run 1
Run 2
(R,R)
(R,L)
(L,R)
(L,L)
1.0
0.9
0.8
0.7
0.6
0.4
0.2
0
100
200
300
Time (min)

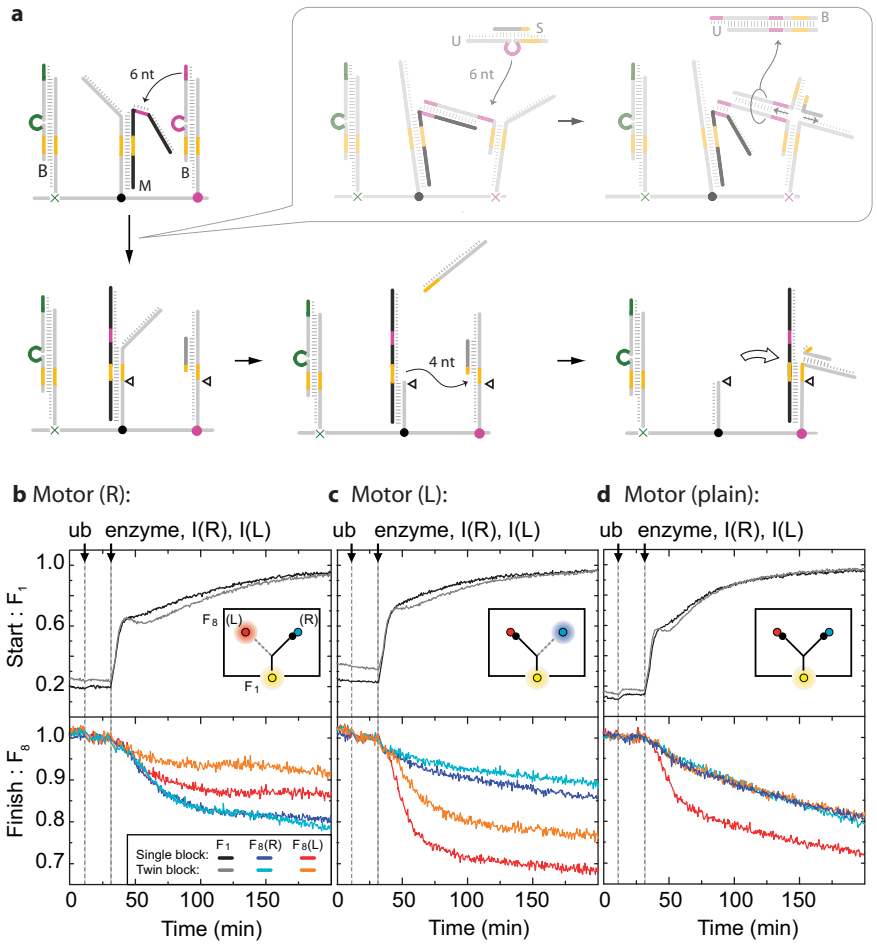
a
6 nt
B
M
B
U
S
6 nt
U
B
4 nt
b Motor (R):
c Motor (L):
d Motor (plain):
ub
enzyme, I(R), I(L)
Start : F1
Finish : F8
1.0
0.6
0.2
1.0
0.9
0.8
0.7
F8 (L)
(R)
F1
Single block:
Twin block:
F1
F8(R)
F8(L)
0
50
100
150
Time (min)